Qeios

https://doi.org/10.32388/2X1GDL

Why Mature Galaxies Seem to have Filled the Universe shortly after the Big Bang

A New Cosmological Model, that Predicted the JWST Observations

May 8, 2023

Arthur E. Pletcher [1]
[1] *International Society for Philosophical Enquiry, Woodbridge, VA, USA*
artpletcher@ultrahighiq.org

Abstract

Recent observations from the first dataset, provided by NASA's James Webb Space Telescope (JWST) of six massive galaxies, at a time in the early universe, seem to defy conventional cosmological models, as they appear to be as mature and developed as our own local group. This article provides a mathematical model, which actually predicted such mature galaxies in a 2022 preprint, prior to these recent observations. As well, this model also predicts discrepancies between theoretical and observed galaxy rotation curves with apparent increased energy density.
The Azimuthal Projection Model of Universe is conceptualized as a $\mathbb{R}^4$ (four spatial) dimensional hypershere, azimuthally projected onto a $\mathbb{R}^3$ (three spatial) dimensional sphere, and is shown to match the Universal expansion rate, as established from supernova cosmology survey points. This parsimonious model requires only a few assumptions, excluding dark energy to satisfy the Cosmological Constant Λ.
This novel model conceives the universe as a higher dimensional dynamic with spacetime as a projection, rather than as an arrow from absolute beginning of the big bang. Red-shifting is alternatively proposed as azimuthal angular projections of wavelengths λ. Accelerated Universal Expansion is alternatively proposed, as azimuthal projections of meridians, asymptotical to a horizon, and Lambert's cosine law of luminous intensity. A radical implication of this model is that azimuthal angular projections are positional dependent, and thus it's conceivable that apparent distances between galaxies vary with the location of the observer (see figure 3). A potential proof is described from the Hubble Tension; Discrepancies between visible spectra red-shifting of cepheid variables (the most recent calculation is $Ho = 74.03 \pm 1.42 km/sec/Mpc$), and from temperature fluctuations in the Cosmic Microwave Background (CMB) (which are calculated to be $Ho = 68.7 \pm 1.3 km/sec/Mpc$), which resolves the discrepancy by recalibrating redshift data from supernova Cosmology survey points.

Keywords dark matter · Hubble tension · galaxy rotation curve · accelerated universal expansion

1 Introduction

This novel conceptual model upends the cosmological timeline, red-shifting, and accelerating universal expansion. It was originally published as a preprint in 2022 [1], prior to the NASA's JWST fist dataset, and predicted the results. This article begins by describing how global meridians, which are azimuthally projected onto a flat surface, are asymptotic along the surface, toward the horizon (away from the observer), in the familiar "Atlas" (gnomonic projected) mapping. By extension, the hypermeridians of a $\mathbb{R}^4$ (four spatial) dimensional hypershere, azimuthally projected onto a $\mathbb{R}^3$ (three spatial) dimensional sphere, are shown to be asymptotic along the spherical surface and also away from the observer. A coordinate system is presented (in a cross section) to equate red-shifting of wavelengths λ with azimuthal angular projections, Using this equation, red-shift (z) is revised from: $z = \frac{\lambda_{obs} - \lambda_{rest}}{\lambda_{rest}}$ to be a function of distance x_n and hyperspere arc length (radian) $z = \frac{\lambda \frac{x_n}{a} - \lambda}{\lambda}$. In conjunction with observed red-shifting survey data and Lambert's cosine law of luminous intensity, the universal hyperspere radius is estimated. From these established parameters, it is shown how both velocity and energy density appear to increase along azimuthally projected (skewed) length (x). As well, how galaxies appear to be dilated (or elongated), along the line of sight, with a resulting flattened rotation curve. From these established parameters, a function is developed to plot a curve, which is superimposed upon graphs (Distance modulus (μ) vs red-shift (z)) of data points from the HST Key Project.
discrepancies between theoretical and observed galaxy rotation curves, as well as apparent increased energy density are shown to be predicted from this model.

2 Azimuthal Projections onto an $\mathbb{R}^2$ Plane Appear to Expand Outward from the Observer, along the plane

Figure 1 shows an observer on a $\mathbb{R}^2$ plane, positioned along a tangent of a $\mathbb{R}^3$ sphere, measures projected meridians at distance x_n, per the equation [2]:

$$x_n = R\ tan(\theta) \tag{1}$$

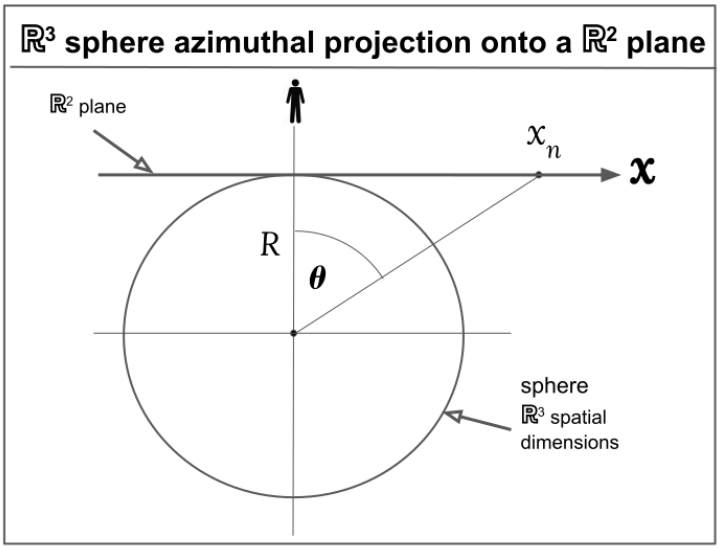

Figure 1: $\mathbb{R}^3$ sphere azimuthally projected onto a $\mathbb{R}^2$ plane. Distance from angle θ and radius of sphere.

Figure 2 shows how azimuthally projected meridians are asymptotic along the $\mathbb{R}^2$ plane, and toward the horizon (away from the observer).

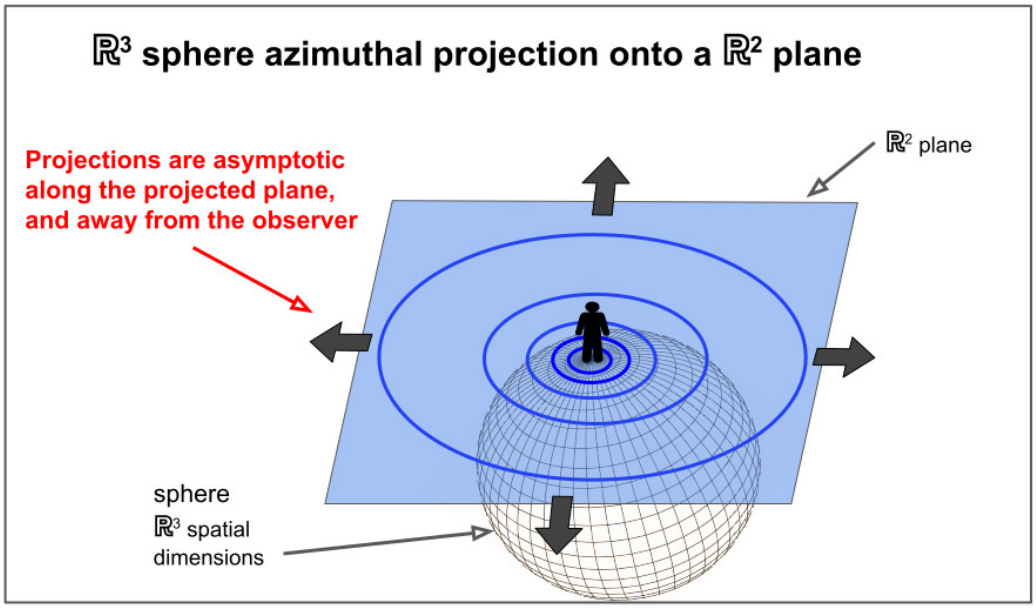

Figure 2: meridians are asymptotic along the $\mathbb{R}^2$ plane, and toward the horizon (away from the observer).

Figure 3 shows how azimuthal projections expansion is relative to the observer's position. On the left side, the observer is positioned along a tangent at projection a, and expansion increases toward point g. However on the right side, the observer is positioned along a tangent at projection g, and expansion increases toward point a.

Positional Dependence of Projection Expansion

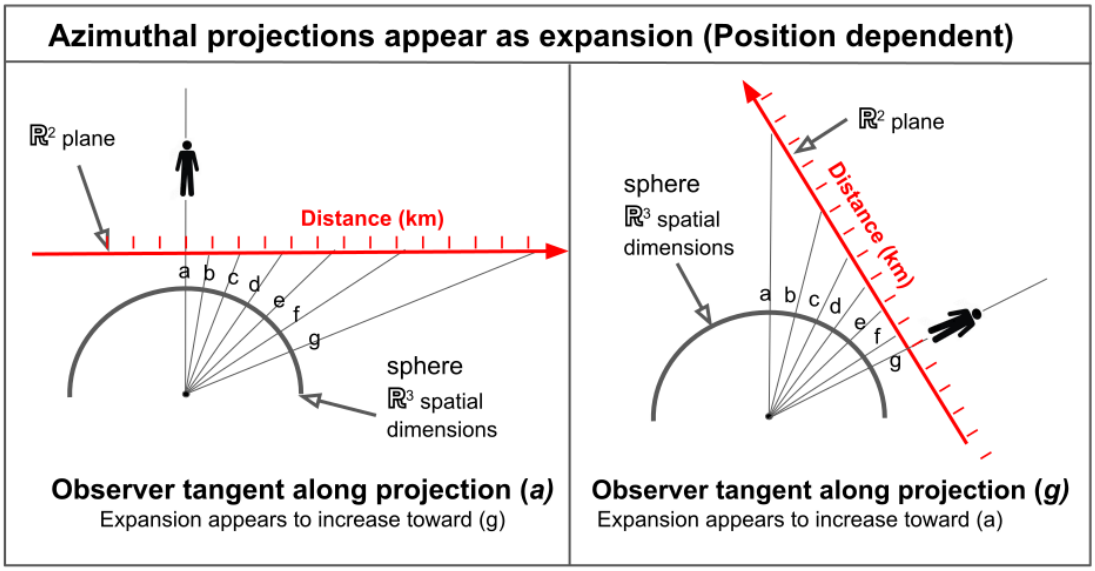

Figure 3: Azimuthal projections appear as expansion (Position dependent)

3 Azimuthal Projections onto an $\mathbb{R}^3$ Sphere Appear to Expand outward from the Observer in three spacial dimensions

Figure 4 shows how azimuthally projected hyper-meridians are asymptotic along the $\mathbb{R}^3$ sphere, and outward from the observer.

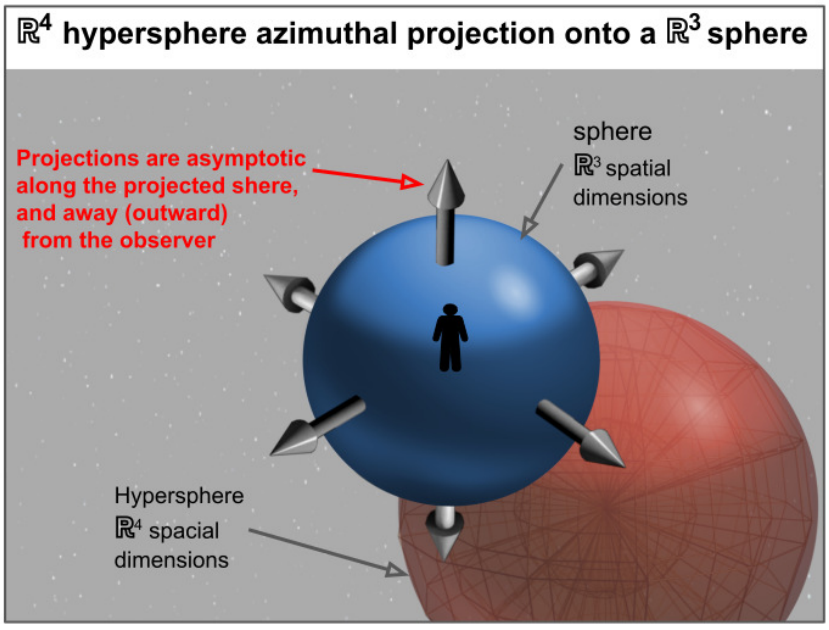

Figure 4: $\mathbb{R}^4$ hypersphere azimuthally projected onto a $\mathbb{R}^3$ sphere. hyper-meridians are projected asymptotic along the sphere, and away from the observer.

Figure 5 shows how azimuthal projections red-shifting is relative to the observer's position. On the left side, the observer is positioned along a tangent at projection a, and red-shifting increases toward point g. However on the right side, the observer is positioned along a tangent at projection g, and red-shifting increases toward point a. A radical implication of this model is that azimuthal angular projections are positional dependent, thus degrees of redshifting over distance is positional dependent. It's conceivable that our local group would appear to be much more expanded, from the perspective of remote observer, and vice versa; vastly remote galaxies would appear to spaced much closer together, from the perspective of a remote observer.

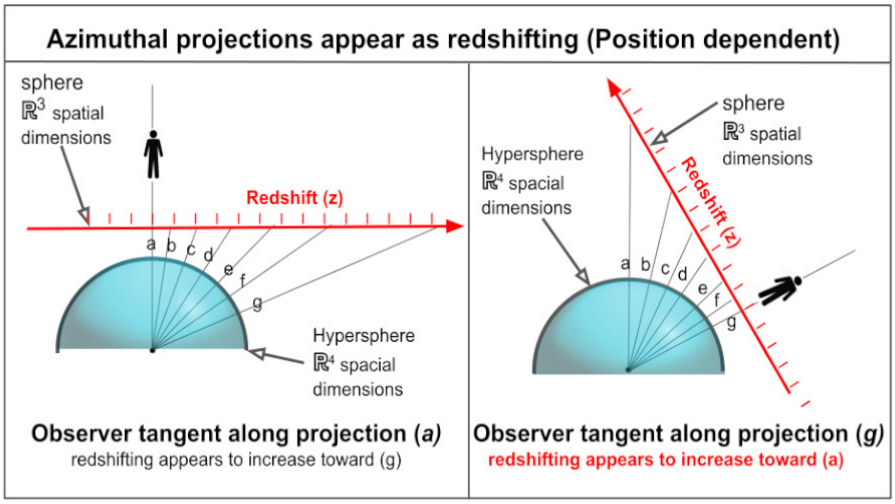

Figure 5: Azimuthal projections appear as red-shifting (Position dependent)

4 Red-shifting is Alternatively Proposed as Azimuthal Angular Projections of Wavelengths λ

As Azimuthal projections are asymptotic along the observer's line of sight, obliqueness increases with distance x. Thus wave lengths become stretched along the observer's line of sight x. The observer in spacetime can not directly observe the projections in hyperspace, and is limited to his line of sight on the x direction. Figure 6 shows how the observer measures the wave lengths λ to be skewed (red-shifted). Section $B-B$, the "at rest" wavelength λ_{rest}, is normal to the hypersheric surface. Oblique view $A-A$ is the "observed" wavelength λ_{obs}, with a skewed (elongated) wavelength.

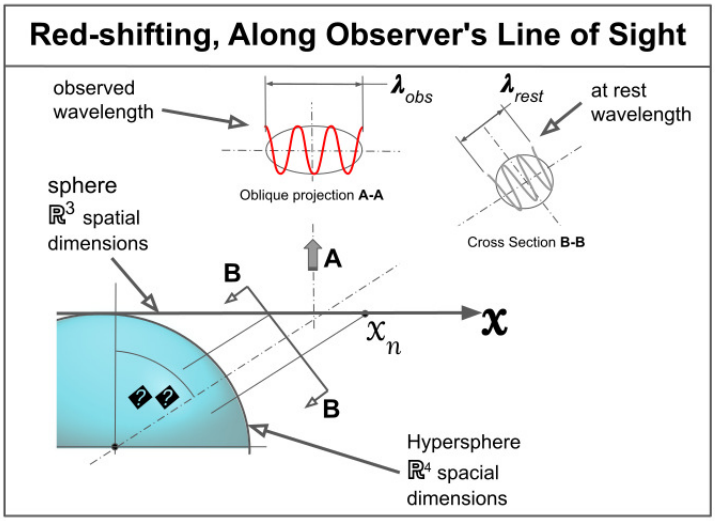

Figure 6: Red-shifting, Along Observer's Line of Sight.

5 Revised Formula for Red-shiff (z)

Figure 7 is a 2 dimensional cross section of an $\mathbb{R}^4$ (spatial dimensions) hypersphere Azimuthal projected onto a $\mathbb{R}^3$ (spatial dimensions) sphere, and extended along X axis into macrospace. A classic space observer resides along the X axis at reference frame: $x = 0$, from which all measurements ($x_n \neq 0$) are skewed projections, asymptotic to the horizon.

$$S \in \mathbb{R}^2 def = (x, y)||\sqrt{x^2 + y^2} = r|| \tag{2}$$

$$F : S \rightarrow /(x)\left[0, x_n\right] \tag{3}$$

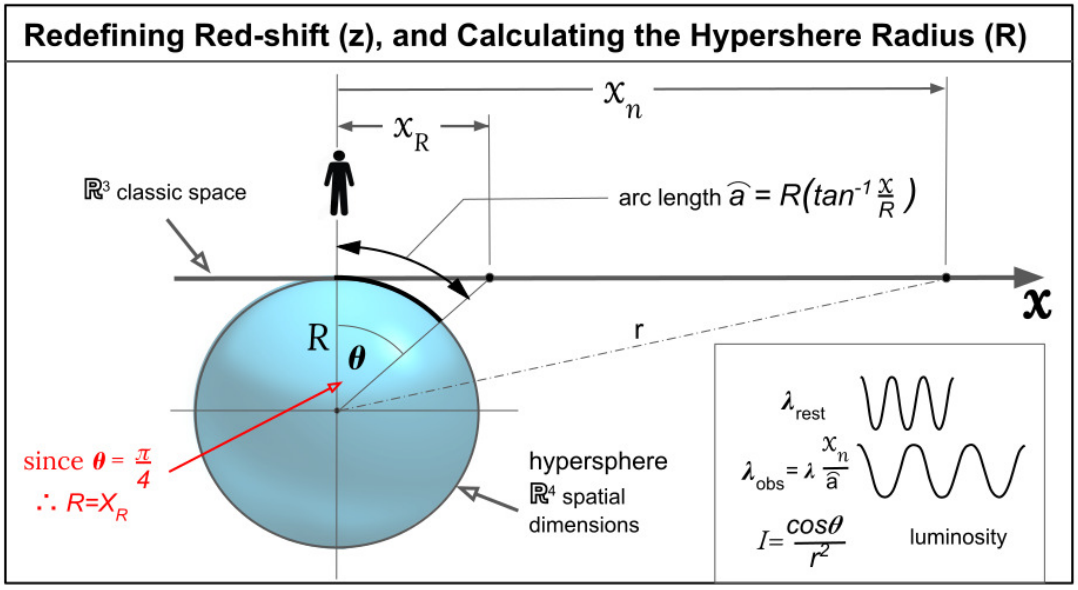

Figure 7: Revised redshift (z), and radius of hypershere

Hyper-meridians and celestial bodies are Azimuthally projected as lateral straight lines, per equation 5:

$$x_n = R\ tan\,\theta$$

Solving for R:

$$R = \frac{x_n}{tan\,\theta} \tag{4}$$

$$\widehat{a} = R\,\theta \implies \tag{5}$$

$$\widehat{a} = R\left(\arctan\frac{x}{R}\right) \tag{6}$$

Framed within this model, electromagnetic wavelengths of λ, along the hypersphere circumference of radius R, are considered to be at rest. However, x_n is projected (skewed) along the X axis and observed with resulting redshift (z), similar to the redshifting equation [3]:

$$z = \frac{\lambda_{obs} - \lambda_{rest}}{\lambda_{rest}} \tag{7}$$

In this alternative model, $\lambda_{obs} = \lambda\frac{x_n}{\widehat{a}}$,

$$z = \frac{\lambda\frac{x_n}{\widehat{a}} - \lambda}{\lambda} \tag{8}$$

Calculating the Universal Hypersphere Radius

The radius R of the hypershere can be deduced from a spacetime perspective (Where humans reside), by considering, that observed **distance (x_R) must be equal to radius R when the tan of θ is equal to 1, or when $\theta = \frac{\pi}{4}$**. Thus from the z value, where $\widehat{a} = R\frac{\pi}{4}$, and $x_R = R$, radius R is derived,

$$\widehat{a} = R\left(\frac{\pi}{4}\right) \qquad Substituting\ \frac{\pi}{4}\ for\ \theta\ in\ equation\ 5 \tag{9}$$

$$z = \frac{\lambda\left(\frac{x_n}{R\frac{\pi}{4}}\right) - \lambda}{\lambda} \qquad Inserting\ into\ equation\ 8 \tag{10}$$

$$z = \frac{x_n}{R\left(\frac{\pi}{4}\right)} - 1 \qquad cancelling\ \lambda \tag{11}$$

$$z = \frac{R}{R\left(\frac{\pi}{4}\right)} - 1 \qquad Since\ x_n = R, \tag{12}$$

$$z = \left(\frac{4}{\pi}\right) - 1 \qquad Simplifies\ to, \tag{13}$$

$$z = 0.273 \tag{14}$$

Finding R from $z = 0.273$, using the approximate distance formula,

$$d \approx \frac{zc}{H_0} \tag{15}$$

At current H_0 value of: $73.8 km/sec/Mpc$

$$R \approx \frac{0.273 * 299792 km/sec}{73.8 km/sec/Mpc} \implies \tag{16}$$

Thus, the radius of the $\mathbb{R}^5$ hypersphere,

$$R \approx 1108.987\ Mpc \tag{17}$$

6 Accelerated Universal Expansion is Alternatively Proposed, as Azimuthal Projections of Meridians, Asymptotical to a Horizon, and Lambert's Cosine law of Luminous Intensity

Velocity Appears to Increase Along Projected Length x_n

In figure 7. Light-waves and energy density are constant along arc length $\widehat{a}$. However from the r.f. of an observer on the projected surface, topology is skewed (elongated). Light-waves travel along X_n with an apparent increased in velocity $\vec{v'}$ of:

$$\frac{\vec{v'}}{\vec{v}} = \frac{X_n}{\widehat{a}} \tag{18}$$

Calculating z per Distance x

Now that R (The radius of the hypersphere) has been established, values of z can be determined from any value of x_n. Note that x_n is a one dimensional cross-section of the space which humans measure galactic distance, although it is actually a skewed projection of hyper-arc length $\widehat{a}$ onto classic space. Thus, from values of distance modulus μ and established radius R, theta is easily determined. Subsequently from theta, $\widehat{a}$ is determined. Finally from equation 8, z is derived at any distance x_n.

Energy Density Increases along Length X_n

Corollary 0.1 *As velocity along skewed x appears to increase per equation 18, energy density ρ proportionally increases, due to increased velocities in particle kinetic and internal energies (compression, energy of nuclear binding, etc.). The observer at $x = 0$ measures volume at x_n [mpc] with increased energy density ρ_n per equation:*

$$\frac{\Delta\rho_n}{\Delta\rho} = \frac{(x_n - R)}{R}$$

Lambert's Cosine Law of Illumination

Consider that figure 7 describes an oblique projection of a source S with an illuminate value I. According to Lambert's Cosine Law of illumination [4], intrinsic values of such projected light will decrease in value with θ per equation:

$$I = \frac{\cos\theta}{r^2} \tag{19}$$

In this model, the luminous intensity of type Ia supernovae would decrease, accordingly. Thus, conventionally accepted standard candle measurements along x, would need to be recalculated per Lambert's Cosine Law.

7 Galaxy Rotation Curve with Increased Density

The discrepancies between theoretical and observed galaxy rotation curves involve both density and velocity. Conventionally, the dependence of circular velocity V_{circ} on radial distance R assumes M, m and velocity to be fixed over large scales in Kepler's law, [5]

$$T^2 = \frac{4\pi^2 r^3}{GM} \Rightarrow T^2 \propto r^3$$

Moreover, gravitational lensing demonstrates the existence of a much greater Mass (density) than the sum of the stars within the galaxy. **However, this alternate model specifically addresses these two issues and provides an alternative explanation,**

Kepler's Law rearranged as density ρ integrated over time dt

Corollary 0.2 *Velocity $\vec{v}$ and density ρ_n are measured with increased magnitude per distance x_n. This directly extends to energy density within galaxies and the effects on rotational velocity, such that: As x_n increases, centripetal force is perfectly balanced by increases in $\vec{v}$ and, subsequently, ρ_n,*

$$\frac{v^2}{r} = \frac{G}{r^2}M = \frac{G}{r^2}\int \rho_n dt$$

Note: total mass M inside the circle of the radius r can be obtained by doing integration of mass density in a volume. $M = \int \rho_n dt$. $\rho = \rho_R$ and ρ_M (Dark components are excluded from this model, with the intent of presenting an alternative).
Figure 9 shows how skewed projected meridians, along the observer's line of sight, appear elongated and are measured with greater density. The result is a flattened rotation curve, per $\frac{x}{a}$. Thus, an elongated galaxy appears to have greater rotational velocity, and energy density.

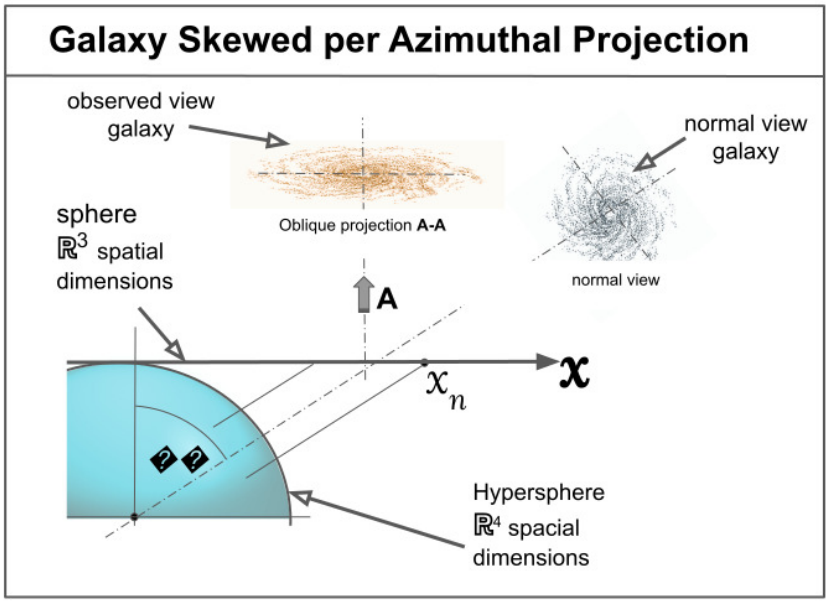

Figure 8: Spiral galaxy projection is skewed

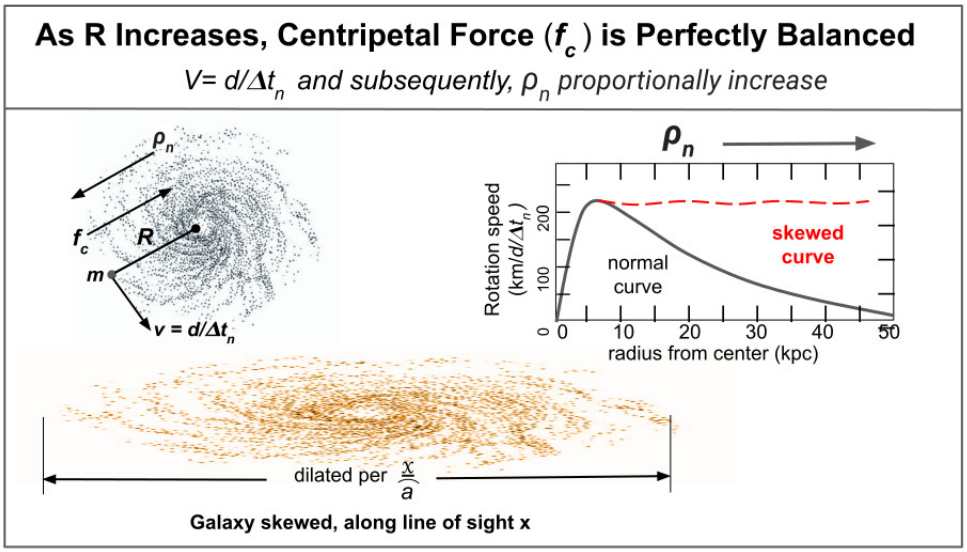

Figure 9: Elongated galaxy appears to have greater rotational velocity, and energy density.

8 Graphing a Function that conforms with the Hubble Diagram

From this model of higher dimensional gnomonic projection, function $F(z)$ provides a graph to compare with Supernova Cosmology Survey Points. Using z as the dependent variable, and μ as independent variable, such that $F(z)$ is a function of μ. From x_n in equation 7, Using equation 6, and converting R to mega parsecs.

$$\lambda X_n = \left(\lambda_{rest} \frac{x}{1108.987\left(\arctan\frac{x}{1108.987}\right)}\right) \tag{20}$$

Inserting into equation 7,

$$z = \left[\frac{\left(\lambda_{rest} \frac{x}{1108.987\left(\arctan\frac{x}{1108.987}\right)}\right) - \lambda_{rest}}{\lambda_{rest}}\right] \tag{21}$$

λ_{rest} cancels, leaving,

$$z = \left[\left(\frac{x}{1108.987\left(\arctan\frac{x}{1108.987}\right)}\right)\right] - 1 \tag{22}$$

Converting redshift z to velocity km/sec,

$$F = \left[\left(\frac{x}{1108.987\left(\arctan\frac{x}{1108.987}\right)}\right) - 1\right] * 300{,}000 km/sec \tag{23}$$

Substituting Lambert's equation (19) for x,

$$F = \left[\left(\frac{x(1108.987 * cos((\arctan(\frac{x}{1108.987}))))}{\left(\frac{cos\left(\left(\arctan\left(\frac{x}{1108.987}\right)\right)\right)}{x^2+1108.987^2}\right)^2 + 1108.987^2}\right) - 1\right] * cK \tag{24}$$

Where K is a slope correction constant, which is necessary to offset conventional measurements of standard candle distances.

Table 1 lists extrapolated points, at $50(Mpc)$ intervals, of Function $F : d \mapsto v \mid F = \{v, f(d)\}[0.000, 5x10^8]$. Also, corresponding values of μ and z

Figure 10 shows the Function $F : d \mapsto v \mid F = \{v, f(d)\}[0.000, 5x10^8]$

Figure 11 shows the Function $F : z \mapsto \mu \mid F = \{\mu, f(z)\}[0.000, 0.125]$. **Note the familiar curve (in logarithmic scale), which is conventionally interpreted as "accelerated expansion".**

Table 1: Extrapolated points of function F. In successive columns:, [pc] (distance parsec), [km/s] (kilometers per second), [μ] (Distance modulus), [z] (redshift),

pc	km/s	μ	z
5.000E+07	4.129E+03	33.495	0.014
1.000E+08	8.228E+03	35.000	0.027
1.500E+08	1.227E+04	35.880	0.041
2.000E+08	1.622E+04	36.505	0.054
2.500E+08	2.006E+04	36.990	0.067
3.000E+08	2.377E+04	37.386	0.079
3.500E+08	2.734E+04	37.720	0.091
4.000E+08	3.074E+04	38.010	0.103
4.500E+08	3.397E+04	38.266	0.113
5.000E+08	3.703E+04	38.495	0.124

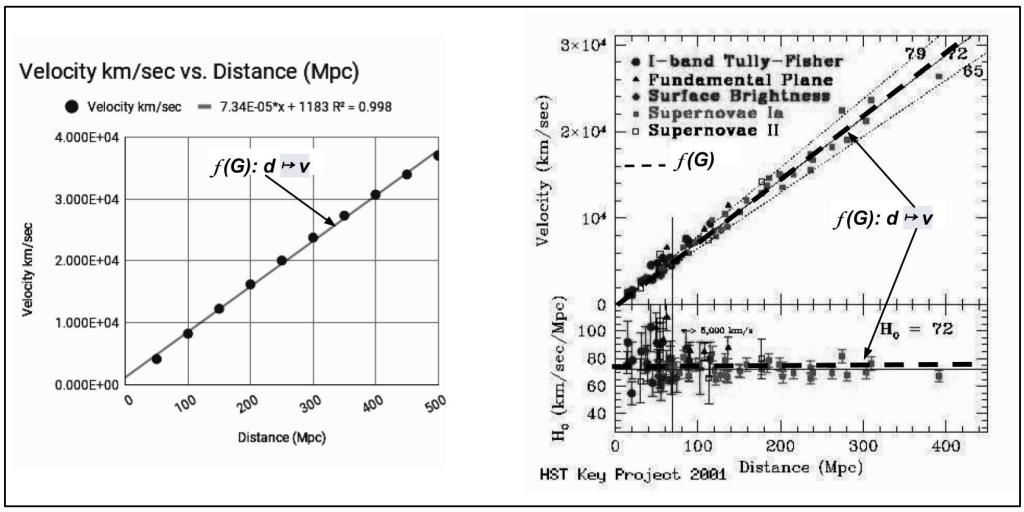

Figure 10: Left: Function $F : d \mapsto v$, with extrapolated points. Right: Function F superimposed onto the HST Key Project

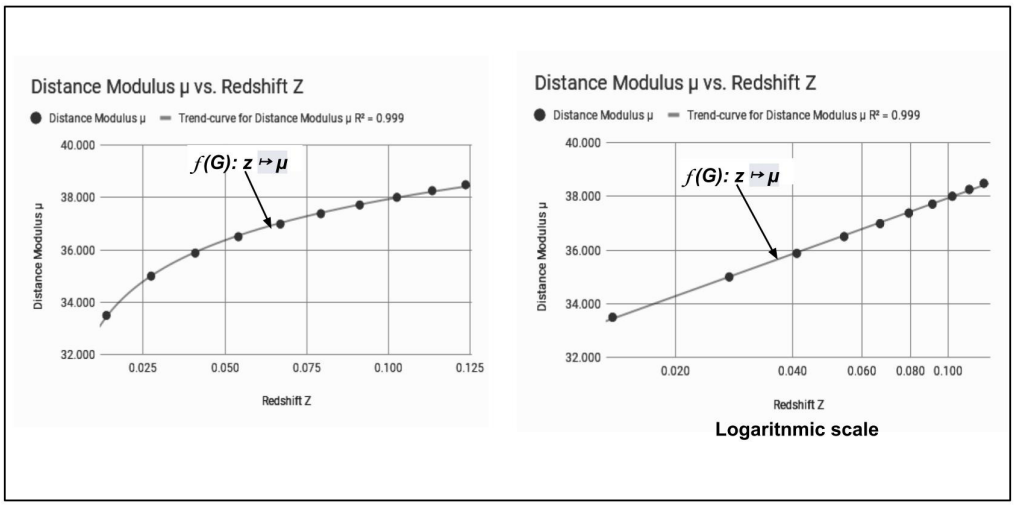

Figure 11: Left: Function $F : z \mapsto \mu$, with extrapolated points. Right: Function F with logarithmic scale, along z axis. **Note the familiar curve, which is conventionally interpreted as "accelerated expansion".**

The Bering Strait Paradox

The familiar Atlas map, which is an $\mathbb{R}^2$ azimuthal global projection, typically places Siberia and Alaska at opposite extremes. However, they are locally connected at the Bering Strait, as viewed in $\mathbb{R}^3$ space. See figure 12.

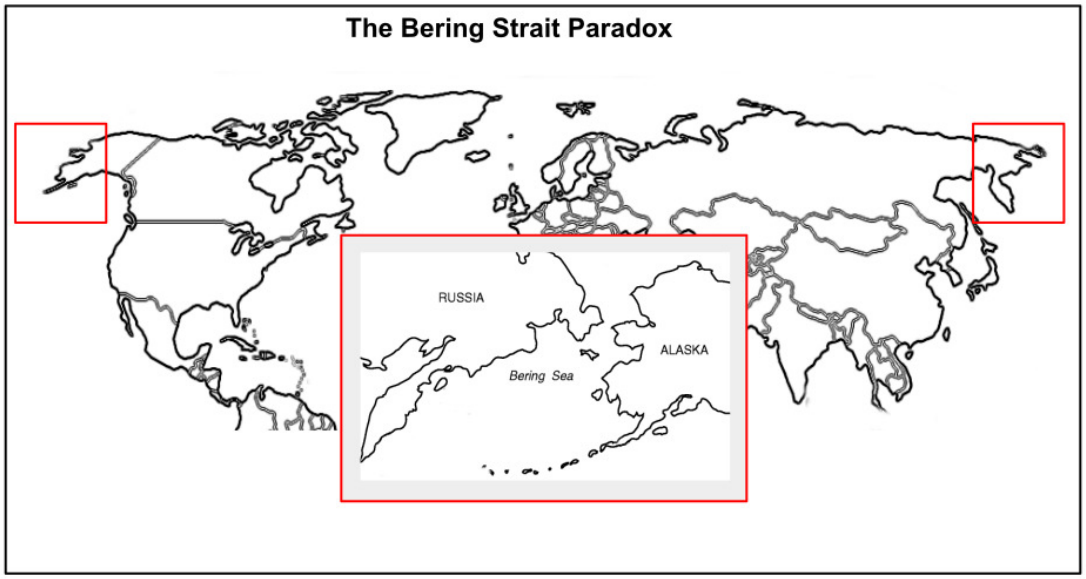

Figure 12: Atlas map, which is an $\mathbb{R}^2$ azimuthal global projection

An analogy, by extension to the Bering Strait paradox is that the extreme $\mathbb{R}^3$ parameters of Macro-space vs micro-space are actually connected in an $\mathbb{R}^4$ torus space. See figure 13.

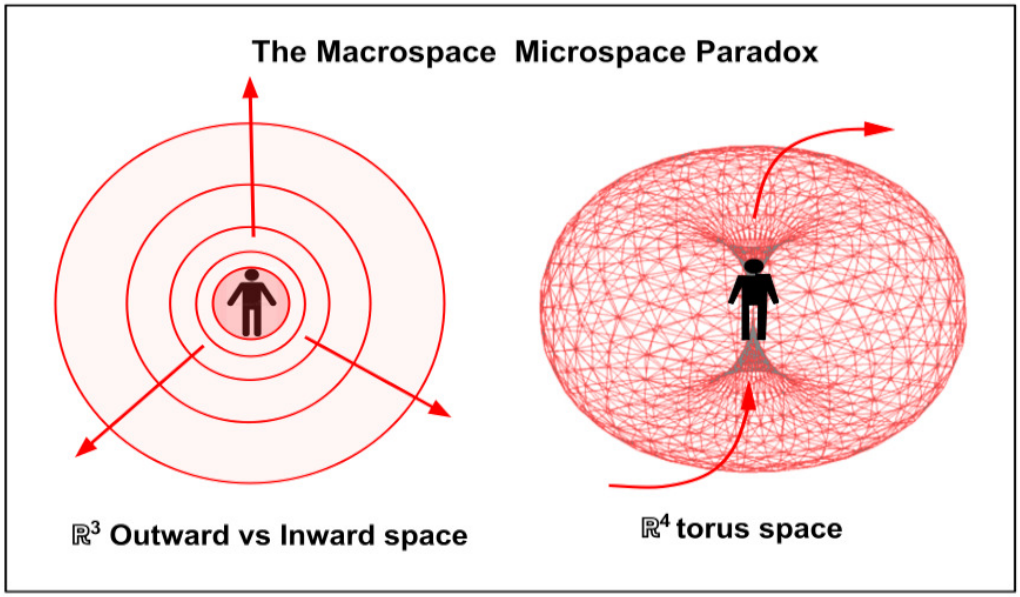

Figure 13: Macro-space vs micro-space are actually connected in an $\mathbb{R}^4$ torus space.

9 The Unit of Time in an $\mathbb{R}^4$ Torus Space

A corollary of the azimuthal projection model of spacetime would be that the unit of time varies with the metric expansion of space w.r.t. the observer. In macro-space, decreasing time units appear equivalent to increasing universal acceleration. In micro-space, increased time units appear as a delayed camera shuttle, such that multiple positions of a particle are observed in a single instant. See "A Fundamental Conservation as a Unification of Quantum Theory and Relativity". [6]

10 Why then do the Most Distant Galaxies Appear Fully Developed?

The James Webb Space Telescope (JWST) observations of the most distant galaxies, some formed just 330 million years after the Big Bang when the universe was a mere 2 percent of its current age, appear as no less developed than our local group. **Consequently, such observations compel theorists to rethink current standard models**. Just as The Azimuthal Projection Model of Universal Expansion implies that our Milky Way galaxy's rotational curve would appear greatly accelerated and flattened from vast distances, it predicts the JWST observations as well. The fundamental concept of this model, is that redshifting is viewer dependent, and a function of projection at any given point. Thus, the radical implication is that the universe must be conceived of as a higher dimensional dynamic with spacetime as a limited projection which is viewer dependent, rather than as an arrow from absolute beginning of the big bang.

11 Proposed Proof of the Azimuthal Projection Model

An ideal proof of comparing red-shift (z) values from vast distances, as in figure 5, is highly unrealistic. However, a significant proof can be derived from discrepancies (rates of expansion over distance) between visible spectra red-shifting of cepheid variables (the most recent calculation is $Ho = 74.03 \pm 1.42 km/sec/Mpc$ [7]), and from temperature fluctuations in the Cosmic Microwave Background (CMB) (which are calculated to be $Ho = 68.7 \pm 1.3 km/sec/Mpc$) [8]. This model predicts that by re-calibrating red-shifting distance ladders with supernova Cosmology Survey Points, and adjusting for Lambert's Cosine Law of illumination (equation 19), the Hubble Constant H_0 from adjusted red-shifting survey data will more closely match the CMB H_0.

12 Conclusion

This parsimonious model, is based solely on a few assumptions. it does not require dark energy to satisfy the Cosmological Constant Λ. It implies a smaller universe than conventional estimates, and the universal hypersphere radius is easily derived. A great many mysteries are resolved, including galaxy rotation curves, accelerated expansion, as well as increased energy density. In summary, it is conceptually more reasonable.

Data Availability Statement: No Data associated in the manuscript

References

[1] A. E. Pletcher. The azimuthal projection model of universal accelerated expansion. DOI: 10.21203/rs.3.rs-2183971/v1, 2022.

[2] Coxeter H. Introduction to Geometry (2). Wiley, Manhattan, 1969.

[3] Taylor E and Wheeler JA. Spacetime Physics. WH Freeman and Company, New York, 1992.

[4] R Waynant. Electro-Optics Handbook. McGraw-Hill, 1994.

[5] Butikov E. Motions of Celestial Bodies. IOP Publishing, Philadelphia, 2014.

[6] A. E. Pletcher. A fundamental conservation as a unification of quantum theory and relativity. DOI: 10.2139/ssrn.3234693, 2022.

[7] Adam Riess. Large magellanic cloud cepheid standards provide a 1% foundation for the determination of the hubble constant and stronger evidence for physics beyond lambdacdm. arXiv:1903.07603, 2019.

[8] Graeme E. Addison. High h0 values from cmb e-mode data: A clue for resolving the hubble tension? arXiv:2102.00028, 2021.